PERGAMON

International Journal of Solids and Structures 40 (2003) 6143–6162

INTERNATIONAL JOURNAL OF SOLIDS and STRUCTURES

www.elsevier.com/locate/ijsolstr

The weight function for cracks in piezoelectrics

Robert McMeeking [a,*], Andreas Ricoeur [b]

[a] *Department of Mechanical and Environmental Engineering and Materials Department, University of California, Santa Barbara, Santa Barbara, CA 93106, USA*

[b] *Institute of Mechanics and Fluid Dynamics, Freiberg University of Mining and Technology, 09596 Freiberg, Germany*

Received 19 July 2002

Abstract

The weight function in fracture mechanics is the stress intensity factor at the tip of a crack in an elastic material due to a point load at an arbitrary location in the body containing the crack. For a piezoelectric material, this definition is extended to include the effect of point charges and the presence of an electric displacement intensity factor at the tip of the crack. Thus, the weight function permits the calculation of the crack tip intensity factors for an arbitrary distribution of applied loads and imposed electric charges. In this paper, the weight function for calculating the stress and electric displacement intensity factors for cracks in piezoelectric materials is formulated from Maxwell relationships among the energy release rate, the physical displacements and the electric potential as dependent variables and the applied loads and electric charges as independent variables. These Maxwell relationships arise as a result of an electric enthalpy for the body that can be formulated in terms of the applied loads and imposed electric charges. An electric enthalpy for a body containing an electrically impermeable crack can then be stated that accounts for the presence of loads and charges for a problem that has been solved previously plus the loads and charges associated with an unsolved problem for which the stress and electric displacement intensity factors are to be found. Differentiation of the electric enthalpy twice with respect to the applied loads (or imposed charges) and with respect to the crack length gives rise to Maxwell relationships for the derivative of the crack tip energy release rate with respect to the applied loads (or imposed charges) of the unsolved problem equal to the derivative of the physical displacements (or the electric potential) of the solved problem with respect to the crack length. The Irwin relationship for the crack tip energy release rate in terms of the crack tip intensity factors then allows the intensity factors for the unsolved problem to be formulated, thereby giving the desired weight function. The results are used to derive the weight function for an electrically impermeable Griffith crack in an infinite piezoelectric body, thereby giving the stress intensity factors and the electric displacement intensity factor due to a point load and a point charge anywhere in an infinite piezoelectric body. The use of the weight function to compute the electric displacement factor for an electrically permeable crack is then presented. Explicit results based on a previous analysis are given for a Griffith crack in an infinite body of PZT-5H poled orthogonally to the crack surfaces.

Keywords: Cracks; Piezoelectrics; Intensity factors; Weight function; Stress; Electric field

* Corresponding author. Tel.: +1-805-893-4583; fax: +1-805-893-8486.
E-mail address: rmcm@engineering.ucsb.edu (R. McMeeking).

0020-7683/$ - see front matter © 2003 Elsevier Ltd. All rights reserved.
doi:10.1016/S0020-7683(03)00366-4

1. Introduction

In an isotropic linear elastic material, the weight function $h_{\mathrm{I}}(x_i^{\mathrm{P}})$ is the Mode I stress intensity factor for a unit point or line load at x_i^{P} (Bueckner, 1970; Rice, 1972). For example, in the plane crack problem depicted in Fig. 1, the Mode I stress intensity factor is a

$$K_{\mathrm{I}} = h_{\mathrm{I}}(x_i^{\mathrm{P}})P_2 \tag{1}$$

where P_2 is interpreted as a line load in this case. In addition, for an isotropic material there is a Mode II stress intensity factor due to the single point load shown in Fig. 1, but we omit this term in our introductory sketch of the weight function. Note, also, that the weight function is generally different for each shape of the body containing a crack. The utility of the weight function is that it can be used to compute the stress intensity factor for an arbitrary distribution of loads. For example, consider tractions $\boldsymbol{T}$ to be applied to the body. The Mode I stress intensity factor due to the T_2 component of these tractions is given by

$$K_{\mathrm{I}} = \int_S h_{\mathrm{I}}(x_i^{\mathrm{P}})T_2(x_i^{\mathrm{P}})\,\mathrm{d}S \tag{2}$$

where S is the surface on which the tractions are applied and $\boldsymbol{x}^{\mathrm{P}}$ is now used to denote the position on the contour S. It should be noted that the T_1 component may in general contribute to K_{I} as well.

Several methods have been given for calculating the weight function for a given problem. Bueckner (1970) obtained the original concept of the weight function from analytic function considerations and later extended his ideas to encompass a work-conjugate integral from which the weight function can be derived (Bueckner, 1973). Rice (1972) showed that the weight function for Mode I problems can be calculated from the displacement solution of any boundary value problem that has a nonzero Mode I stress intensity factor and by extension other modes can be developed in the same manner. These results arise from Maxwell relationships among dependent and independent variables. Consequently, differentiation of the displacement solutions with respect to the crack length along with some further manipulations provides the desired results. Other methods exist for calculating the weight function. For example, Paris and McMeeking (1975) and Paris et al. (1976) developed a computational technique using finite elements to calculate the weight

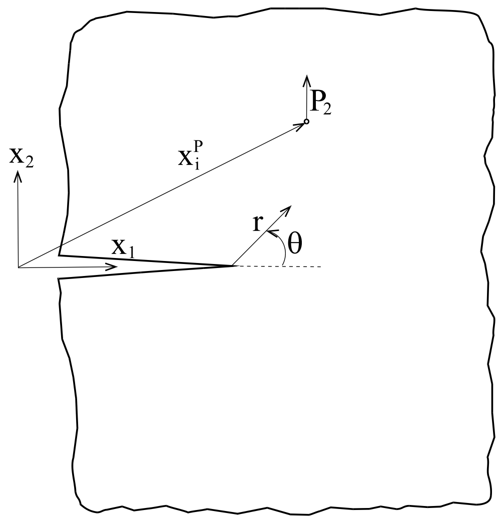

Fig. 1. A crack in a plane body with a single line load P_2.

function directly by imposing tractions on a cut-out surface around the crack tip. Labbens et al. (1975) and Labbens et al. (1976) produced a similar numerical technique and applied it to three-dimensional crack problems. Parks and Kamenetzky (1979) and Vanderglas (1978) have used virtual crack extension methods to provide other algorithms.

The weight function is of considerable utility since it provides a universal form for calculation of crack tip intensity factors once it has been established. Thus, the intensity factors for any distribution of loads can be calculated from an established weight function. In addition, there are special applications of the weight function that are very useful, such as the calculation of the effect of bridging tractions on a crack surface due to fibers or friction between grains in contact across the crack (Evans and McMeeking, 1986; Marshall et al., 1985). Furthermore, Rice's (1972) derivation of the weight function shows that once any crack problem with specific loading is completely solved to give its physical displacements, the weight function can then be formulated and the stress intensity factors for any other applied load for the body in question can then be computed. These advantages make it highly desirable to have the weight function formulated for a piezoelectric material using the methodology of Rice (1972). Such a formulation will extend the weight function to encompass the effect of imposed electric charges and to allow calculation of the crack tip electric displacement intensity factor (Suo et al., 1992).

Thus, the method of Rice (1972) will be used in this paper to formulate the weight function for a crack in a piezoelectric material. In this case, the material is anisotropic and point forces and point charges in general will give rise to Mode I, II and III stress intensity factors and also to an electric displacement intensity factor. It should be noted that previously the weight function was formulated for a piezoelectric material by Ma and Chen (2001) who used Bueckner's (1973) work-conjugate integral and treated the case of an interface crack between two unlike piezoelectric materials. In their work, Ma and Chen (2001) provided generic formulae for the weight function but gave no specific results. In the current paper not only do we provide a more transparent and useful derivation of the weight function than that of Ma and Chen (2001) but also we present some specific results for a Griffith crack in PZT-5H to illustrate its utility.

2. Formulation of the weight function for a crack in a piezoelectric material

The derivation of the weight function will be demonstrated through the specific example of the solution for a Griffith crack of length l in a homogeneous material subject to loadings at infinity, as shown in Fig. 2. However, it should be noted that the weight function may be derived for any geometry containing a crack starting with any complete solution to a boundary value problem for that geometry (Rice, 1972). Therefore, that which is given below will provide a template for what has to be done for an arbitrary problem.

The solution to a Griffith crack subject to uniform loading at infinity, as shown in Fig. 2 and known as "Problem 1", involves results at infinity given by

$$\{U\} = \begin{Bmatrix} u_1^\infty \\ u_2^\infty \\ u_3^\infty \\ \phi^\infty \end{Bmatrix} \tag{3}$$

where u_i^∞ is the displacement at infinity in the x_i-direction and ϕ^∞ is the electric potential at infinity. Formally, these results are infinite, but they can be made finite by considering only the amount caused by introduction of the crack, thereby eliminating the infinite displacements and potential of an infinite uncracked body loaded uniformly at infinity. The crack in this problem is a mathematical slit along the x_1-axis with boundary conditions on its surface given by

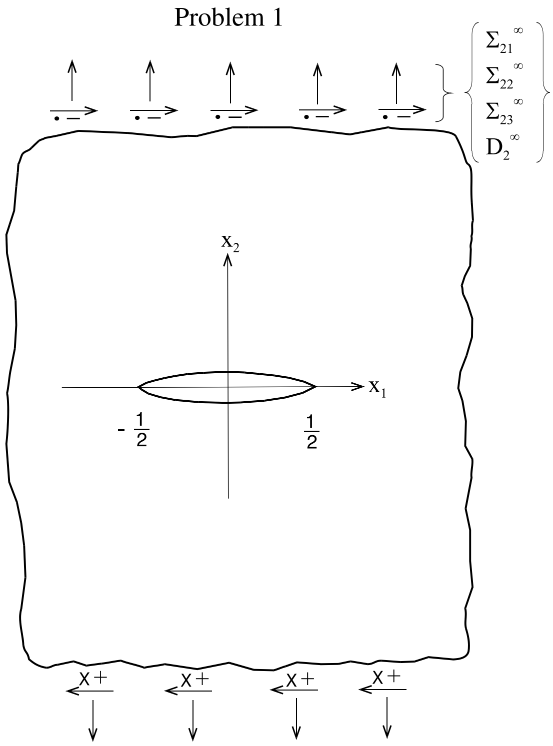

Fig. 2. A Griffith crack of length l with uniform stress Σ_{ij}^{∞} and electric displacement D_2^{∞} applied at infinity, constituting Problem 1.

$$\begin{Bmatrix} \Sigma_{21} \\ \Sigma_{22} \\ \Sigma_{23} \\ D_2 \end{Bmatrix} = 0 \tag{4}$$

where Σ_{ij} is the stress tensor and D_i is the electric displacement. Clearly the surfaces of the crack are traction free. In addition, Eq. (4) implies that the crack is impermeable to the electric field, which is an unphysical condition. This should not be taken to mean that we believe that the impermeable crack is a reasonable model of reality; rather we use the impermeable crack solution as a convenience and we will address the question of the permeable crack once we have obtained the weight function.

Obviously for a complete solution, the displacements and the potential everywhere will be known, but we leave this concept for later. As illustrated in Fig. 2, the loading at infinity is

$$\{\Sigma^{\infty}\} = \begin{Bmatrix} \Sigma_{21}^{\infty} \\ \Sigma_{22}^{\infty} \\ \Sigma_{23}^{\infty} \\ D_2^{\infty} \end{Bmatrix} \tag{5}$$

where Σ_{ij}^{∞} is the stress tensor at infinity and D_i^{∞} is the electric displacement at infinity. The intensity factors for any homogeneous, piezoelectric material in Problem 1 are given by Suo et al. (1992).

$$\begin{Bmatrix} K_{II}^1 \\ K_I^1 \\ K_{III}^1 \\ K_D^1 \end{Bmatrix} = \begin{Bmatrix} \Sigma_{21}^\infty \\ \Sigma_{22}^\infty \\ \Sigma_{23}^\infty \\ D_2^\infty \end{Bmatrix} \sqrt{\pi l/2} \tag{6}$$

where K_{II} is the Mode II stress intensity factor, K_I is the Mode I stress intensity factor, K_{III} is the Mode III stress intensity factor and K_D is the electric displacement intensity factor. The definition of the intensity factors is quite conventional; on the x_1-axis ahead of a right-hand crack tip such as that shown for Problem 1 (Fig. 2), the stress and the electric displacement are given in general to leading order by (Suo et al., 1992)

$$\begin{Bmatrix} \Sigma_{21} \\ \Sigma_{22} \\ \Sigma_{23} \\ D_2 \end{Bmatrix} = \begin{Bmatrix} K_{II} \\ K_I \\ K_{III} \\ K_D \end{Bmatrix} \frac{1}{\sqrt{2\pi\left(x_1 - \frac{l}{2}\right)}} \tag{7}$$

Note that the superscripts 1 in Eq. (6) indicate that these intensity factors pertain to Problem 1.

A second problem is now introduced, illustrated in Fig. 3 and known as "Problem 2". This is the one for which we wish to compute the stress intensity factors and the electric displacement intensity factor. It involves the same Griffith crack of length l as used for Problem 1 and the same piezoelectric material, but now loaded only by a line force P_i^2 at position $\hat{x}_i$ and a collocated line of charges Q^2. The crack surfaces are taken to be free of traction and to be such that D_2 is zero on them as well, meaning that this crack is impermeable as well. As before, this does not mean that we accept that an impermeable crack is realistic, but rather we will construct its weight function and then use it to address the question of a permeable crack.

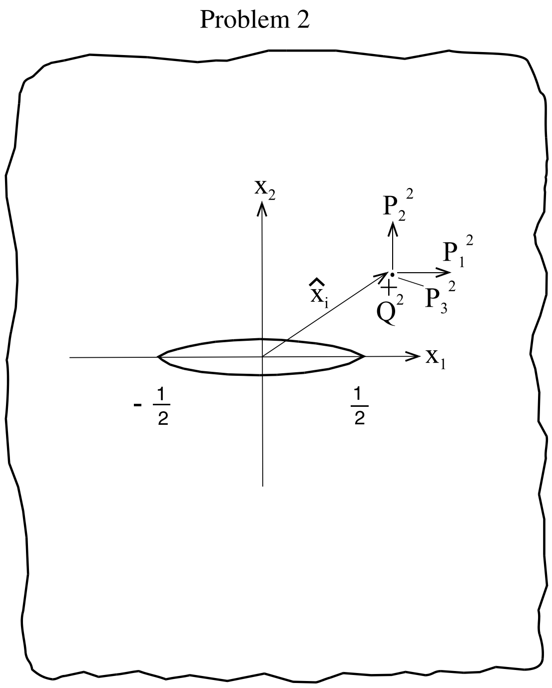

Fig. 3. The same body with a crack as in Fig. 2 with line loads P_i^2 and a line charge Q^2, constituting Problem 2.

The intensity factors due to the line load and charge of Problem 2 are given by

$$\begin{Bmatrix} K_{\mathrm{II}}^2 \\ K_{\mathrm{I}}^2 \\ K_{\mathrm{III}}^2 \\ K_{\mathrm{D}}^2 \end{Bmatrix} = [k(\hat{x}_i, l)] \begin{Bmatrix} P_1^2 \\ P_2^2 \\ P_3^2 \\ -Q^2 \end{Bmatrix} \tag{8}$$

where $[k(\hat{x}_i, l)]$ is a matrix containing the weight functions that we wish to formulate. The reason for using the negative sign in conjunction with the charge will become apparent below. The superscripts 2 in Eq. (8) indicate, of course, that these expressions are for Problem 2.

We now construct a combined problem as illustrated in Fig. 4 by simultaneously imposing the mechanical and electrical loading at infinity of Problem 1 and the line load and charge of Problem 2. As a result of the combined loads, the solution at infinity becomes

$$\begin{Bmatrix} u_1^\infty \\ u_2^\infty \\ u_3^\infty \\ \phi^\infty \end{Bmatrix} = [C^1(l)] \begin{Bmatrix} \Sigma_{21}^\infty \\ \Sigma_{22}^\infty \\ \Sigma_{23}^\infty \\ D_2^\infty \end{Bmatrix} + [C^{12}(\hat{x}_i, l)] \begin{Bmatrix} P_1^2 \\ P_2^2 \\ P_3^2 \\ -Q^2 \end{Bmatrix} \tag{9}$$

where $[C^1]$ is the symmetric generalized compliance matrix for Problem 1 and $[C^{12}]$ is the generalized cross-compliance matrix that gives the displacements and potential due to the loadings of Problem 2 at the location where the loads of Problem 1 are applied; i.e. at infinity. Note that the geometric dependencies of

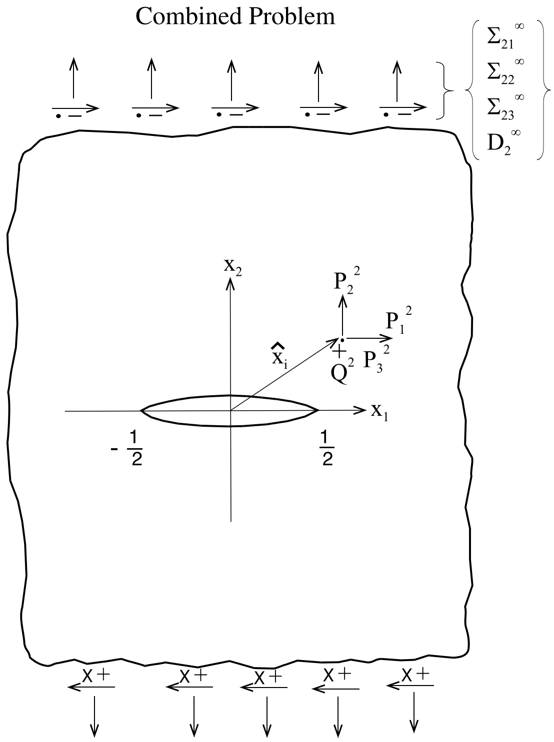

Fig. 4. The same body with a crack as in Figs. 2 and 3 with both stress and electric displacement at infinity and a line load and line charge, constituting the Combined Problem.

the compliance matrices are indicated. In addition, they will depend on the elastic, piezoelectric and dielectric properties of the material, but that has not been indicated explicitly. The conjugate relationship is

$$\begin{Bmatrix} u_1(\hat{x}_i) \\ u_2(\hat{x}_i) \\ u_3(\hat{x}_i) \\ \phi(\hat{x}_i) \end{Bmatrix} = [C^{12}(\hat{x}_i, l)]^{\mathrm{T}} \begin{Bmatrix} \Sigma_{21}^{\infty} \\ \Sigma_{22}^{\infty} \\ \Sigma_{23}^{\infty} \\ D_2^{\infty} \end{Bmatrix} + [C^2(\hat{x}_i, l)] \begin{Bmatrix} P_1^2 \\ P_2^2 \\ P_3^2 \\ -Q^2 \end{Bmatrix} \tag{10}$$

where the left-hand side gives the displacements and potential at $\hat{x}_i$, the location where the loads of Problem 2 are applied and $[C^2]$ is the symmetric generalized compliance matrix for Problem 2. The symmetries of the generalized compliance matrices for Problems 1 and 2 and the use of the transpose in Eq. (10) of the generalized cross-compliance matrix from Eq. (9) is dictated by the energy considerations that give rise to classical Maxwell relationships.

The electric enthalpy for the combined problem is then given by

$$\psi = \frac{1}{2} \begin{Bmatrix} \Sigma_{21}^{\infty} \\ \Sigma_{22}^{\infty} \\ \Sigma_{23}^{\infty} \\ D_2^{\infty} \end{Bmatrix}^{\mathrm{T}} [C^1] \begin{Bmatrix} \Sigma_{21}^{\infty} \\ \Sigma_{22}^{\infty} \\ \Sigma_{23}^{\infty} \\ D_2^{\infty} \end{Bmatrix} + \begin{Bmatrix} \Sigma_{21}^{\infty} \\ \Sigma_{22}^{\infty} \\ \Sigma_{23}^{\infty} \\ D_2^{\infty} \end{Bmatrix}^{\mathrm{T}} [C^{12}] \begin{Bmatrix} P_1^2 \\ P_2^2 \\ P_3^2 \\ -Q^2 \end{Bmatrix} + \frac{1}{2} \begin{Bmatrix} P_1^2 \\ P_2^2 \\ P_3^2 \\ -Q^2 \end{Bmatrix}^{\mathrm{T}} [C^2] \begin{Bmatrix} P_1^2 \\ P_2^2 \\ P_3^2 \\ -Q^2 \end{Bmatrix} \tag{11}$$

For notational convenience, we introduce $\Sigma_{24}^{\infty} = D_2^{\infty}$, $P_4^2 = -Q^2$, $u_4^{\infty} = \phi^{\infty}$ and $u_4(\hat{x}_i) = \phi(\hat{x}_i)$. It can then be shown that

$$u_i^{\infty} = \frac{\partial \psi}{\partial \Sigma_{2i}^{\infty}} \tag{12}$$

and

$$u_i(\hat{x}_i) = \frac{\partial \psi}{\partial P_i^2} \tag{13}$$

Furthermore, the crack tip energy release rate for propagation of the crack by extension at the right-hand tip is

$$G = \frac{\partial \psi}{\partial l} \tag{14}$$

A second differentiation of Eqs. (13) and (14) gives the Maxwell relationships

$$\frac{\partial G}{\partial P_i^2} = \frac{\partial u_i(\hat{x}_j)}{\partial l} \tag{15}$$

Now we can introduce the Irwin relationship (Suo et al., 1992) for the combined problem as

$$G = \left(\begin{Bmatrix} \Sigma_{21}^{\infty} \\ \Sigma_{22}^{\infty} \\ \Sigma_{23}^{\infty} \\ D_2^{\infty} \end{Bmatrix} \sqrt{\pi l/2} + [k(\hat{x}_i, l)] \begin{Bmatrix} P_1^2 \\ P_2^2 \\ P_3^2 \\ -Q^2 \end{Bmatrix} \right)^{\mathrm{T}} [H] \left(\begin{Bmatrix} \Sigma_{21}^{\infty} \\ \Sigma_{22}^{\infty} \\ \Sigma_{23}^{\infty} \\ D_2^{\infty} \end{Bmatrix} \sqrt{\pi l/2} + [k(\hat{x}_i, l)] \begin{Bmatrix} P_1^2 \\ P_2^2 \\ P_3^2 \\ -Q^2 \end{Bmatrix} \right) \tag{16}$$

where $[H]$ is the symmetric, non-singular Irwin matrix for computing the energy release rate from the intensity factors (Suo et al., 1992). Differentiation of this equation gives

$$\begin{Bmatrix} \frac{\partial G}{\partial P_1^2} \\ \frac{\partial G}{\partial P_2^2} \\ \frac{\partial G}{\partial P_3^2} \\ \frac{\partial G}{\partial P_4^2} \end{Bmatrix} = 2[k(\hat{x}_i, l)]^{\mathrm{T}}[H]\left(\begin{Bmatrix} \Sigma_{21}^{\infty} \\ \Sigma_{22}^{\infty} \\ \Sigma_{23}^{\infty} \\ D_2^{\infty} \end{Bmatrix}\sqrt{\pi l/2} + [k(\hat{x}_i, l)]\begin{Bmatrix} P_1^2 \\ P_2^2 \\ P_3^2 \\ P_4^2 \end{Bmatrix}\right) \tag{17}$$

Similarly, differentiation of Eq. (10) provides

$$\begin{Bmatrix} \frac{\partial u_1(\hat{x}_i)}{\partial l} \\ \frac{\partial u_2(\hat{x}_i)}{\partial l} \\ \frac{\partial u_3(\hat{x}_i)}{\partial l} \\ \frac{\partial u_4(\hat{x}_i)}{\partial l} \end{Bmatrix} = \left(\frac{\partial}{\partial l}[C^{12}(\hat{x}_i, l)]^{\mathrm{T}}\right)\begin{Bmatrix} \Sigma_{21}^{\infty} \\ \Sigma_{22}^{\infty} \\ \Sigma_{23}^{\infty} \\ \Sigma_{24}^{\infty} \end{Bmatrix} + \left(\frac{\partial}{\partial l}[C^2]\right)\begin{Bmatrix} P_1^2 \\ P_2^2 \\ P_3^2 \\ P_4^2 \end{Bmatrix} \tag{18}$$

Now set P_i^2 to zero and use Eq. (15) to obtain

$$2\sqrt{\pi l/2}[k(\hat{x}_i, l)]^{\mathrm{T}}[H]\begin{Bmatrix} \Sigma_{21}^{\infty} \\ \Sigma_{22}^{\infty} \\ \Sigma_{23}^{\infty} \\ \Sigma_{24}^{\infty} \end{Bmatrix} = \left(\frac{\partial}{\partial l}[C^{12}(\hat{x}_i, l)]^{\mathrm{T}}\right)\begin{Bmatrix} \Sigma_{21}^{\infty} \\ \Sigma_{22}^{\infty} \\ \Sigma_{23}^{\infty} \\ \Sigma_{24}^{\infty} \end{Bmatrix} \tag{19}$$

which is valid for arbitrary values of Σ_{ij}^{∞}. Therefore, the stress vector can be eliminated and since $[H]$ is non-singular and symmetric, we obtain

$$[k(\hat{x}_i, l)] = \frac{1}{2\sqrt{\pi l/2}}[H]^{-1}\frac{\partial}{\partial l}[C^{12}(\hat{x}_i, l)] \tag{20}$$

It should be noted that we chose to derive the weight function for a specific geometry (the Griffith crack) starting from a specific loading configuration used as Problem 1 (uniform load at infinity). However, the conceptual steps of the derivation that we used are applicable to any geometry and can be done with any exact solution used as the source for Problem 1. Thus, as in Rice's (1972) derivation of the weight function, Eq. (20) shows that it is proportional to the derivative with respect to crack length of the generalized displacements due to unit loading in any exact solution to a crack problem. As a consequence, the formula given in Eq. (20) states the weight function for any planar geometry containing a through crack in a homogeneous piezoelectric material loaded by line loads and line charges. Furthermore, the result can be extended to 3-dimensional bodies containing cracks of arbitrary shape following Parks and Kamenetzky (1979).

3. The weight function for a Griffith crack in a piezoelectric solid

The impermeable Griffith crack problem in a homogeneous piezoelectric material as shown in Fig. 2 is solved by the expression (Suo et al., 1992).

$$\begin{Bmatrix} u_1(x_i) \\ u_2(x_i) \\ u_3(x_i) \\ \phi(x_i) \end{Bmatrix} = \Re([A][Z][N])\begin{Bmatrix} \Sigma_{21}^{\infty} \\ \Sigma_{22}^{\infty} \\ \Sigma_{23}^{\infty} \\ D_2^{\infty} \end{Bmatrix} \tag{21}$$

where $\Re(\ )$ indicates the real part of the term contained in the parenthesis and $[A]$ and $[N]$ are matrices of complex constants arising in an eigenvalue problem ensuring satisfaction of the governing equations for any homogeneous piezoelectric material (Eshelby et al., 1953; Suo et al., 1992). These matrices are given in

Appendix A for the material PZT-5H. The remaining matrix $[Z]$ in Eq. (21) is formulated following examples given by Suo et al. (1992), Park and Sun (1995), Kemmer (2000) and Kuna and Ricoeur (2002) and is given by

$$[Z] = \begin{bmatrix} \sqrt{z_1^2 - \frac{l^2}{4}} - z_1 & 0 & 0 & 0 \\ 0 & \sqrt{z_2^2 - \frac{l^2}{4}} - z_2 & 0 & 0 \\ 0 & 0 & \sqrt{z_3^2 - \frac{l^2}{4}} - z_3 & 0 \\ 0 & 0 & 0 & \sqrt{z_4^2 - \frac{l^2}{4}} - z_4 \end{bmatrix} \tag{22}$$

with

$$z_i = x_1 + p_i x_2 \tag{23}$$

where p_i are the four complex eigenvalues for the problem mentioned above. These eigenvalues are given in Appendix A for PZT-5H. Note that the term given by Eq. (22) is the part due to the introduction of the crack. The complete solution is obtained by adding the displacements and potential compatible with the uniform strain arising in an infinite body subject to the uniform loading. As a consequence, the displacements appearing in Eq. (21) are finite. However, these displacements are suitable for constructing the weight function, because the additional term connected to the uniform strain is, of course, independent of the crack size. Note that the matrices $[A]$ and $[N]$ correspond to terms that are given the equivalent symbol in the work of Kuna and Ricoeur (2002) where more detail of the solution procedure can be found. The same solution methodology has been used by Suo et al. (1992), Park and Sun (1995) and Kuna and Ricoeur (2002) and variants of it are found elsewhere such as used by Kemmer (2000).

Comparison of Eq. (10) with Eq. (21) shows that, to the neglect of the displacements in the body without a crack

$$[C^{12}]^{\mathrm{T}} = \Re([A][Z][N]) \tag{24}$$

Thus, from Eq. (20), we find that the weight function for the impermeable Griffith crack is

$$[k] = \frac{-1}{4\sqrt{\pi l/2}}[H]^{-1}\Re([A][\widehat{Z}][N])^{\mathrm{T}} \tag{25}$$

where

$$[\widehat{Z}] = \begin{bmatrix} \sqrt{\frac{z_1 + l/2}{z_1 - l/2}} & 0 & 0 & 0 \\ 0 & \sqrt{\frac{z_2 + l/2}{z_2 - l/2}} & 0 & 0 \\ 0 & 0 & \sqrt{\frac{z_3 + l/2}{z_3 - l/2}} & 0 \\ 0 & 0 & 0 & \sqrt{\frac{z_4 + l/2}{z_4 - l/2}} \end{bmatrix} \tag{26}$$

is computed from $[Z]$ according to Eqs. (20) and (21). For points on the crack surface, all z_i are equal to x_1, so the weight function becomes

$$[k] = \frac{\pm 1}{4\sqrt{\pi l/2}}\sqrt{\frac{l/2 + x_1}{l/2 - x_1}}[H]^{-1}\Re(\mathrm{i}[A][N])^{\mathrm{T}} \tag{27}$$

The positive and negative signs in Eq. (27) appear because

$$z_i - \frac{l}{2} = \left(\frac{l}{2} - x_1\right)\mathrm{e}^{\pm \mathrm{i}\pi} \tag{28}$$

on the crack surfaces with the positive sign for the upper crack surface and the negative sign on the lower crack surface whereas

$$z_i + \frac{l}{2} = \frac{l}{2} + x_1 \tag{29}$$

on both crack surfaces. Thus in Eq. (27), the positive sign is used on the upper crack surface and the negative sign is used on the lower crack surface. Eq. (27) is simplified by use of (Suo et al., 1992),

$$[H] = \frac{1}{2}\Re(\mathrm{i}[A][N]) \tag{30}$$

and since $[H]$ is symmetric, the weight function on the crack is

$$[k] = \frac{\pm 1}{2\sqrt{\pi l/2}}\sqrt{\frac{l/2 + x_1}{l/2 - x_1}}[I] \tag{31}$$

Thus the weight function on the surface of the Griffith crack is the same in all homogeneous piezoelectric materials, the anisotropy notwithstanding. Given the result for stress intensity factors in Eq. (6), this latter point is not surprising since uniform 3-dimensional tractions and uniform charge densities on the upper and lower surfaces of the crack with the appropriate signs must lead to Eq. (6) when combined with Eqs. (8) and (31) and integrated in the manner indicated in Eq. (2). Note also that Eq. (31) is consequently valid for an isotropic material that is therefore without piezoelectricity and thus where the dielectricity decouples from the elasticity.

Now return to the general result in Eq. (25) and consider the asymptotic form very close to the right-hand crack tip. In the polar coordinate system based on the right-hand crack tip and shown in Fig. 1, the variable z_i is replaced by

$$z_i = \frac{l}{2} + r(\cos\theta + p_i \sin\theta) \tag{32}$$

Then in the limit $r \to 0$, the weight function becomes

$$[k] = \frac{-1}{\sqrt{8\pi r}}[H]^{-1}\Re([A][\widetilde{Z}][N])^{\mathrm{T}} \tag{33}$$

where

$$[\widetilde{Z}] = \begin{bmatrix} \frac{1}{\sqrt{\cos\theta + p_1 \sin\theta}} & 0 & 0 & 0 \\ 0 & \frac{1}{\sqrt{\cos\theta + p_2 \sin\theta}} & 0 & 0 \\ 0 & 0 & \frac{1}{\sqrt{\cos\theta + p_3 \sin\theta}} & 0 \\ 0 & 0 & 0 & \frac{1}{\sqrt{\cos\theta + p_4 \sin\theta}} \end{bmatrix} \tag{34}$$

A similar treatment of Eq. (31) gives the near tip weight function for the right-hand crack tip on the crack surface to be

$$[k] = \frac{\pm 1}{\sqrt{2\pi r}}[I] \tag{35}$$

Note that the Irwin matrix $[H]$ is given in Appendix A for PZT-5H.

4. Results

The use and character of the weight function for a piezoelectric will now be demonstrated through results from examples. First, we will use the expression in Eq. (31), which is valid for any material. Consider the problem illustrated in Fig. 5 in which there are mechanical loads and charges applied at infinity and mechanical loads and charges imposed on the crack surface. The loads and charges at infinity are in equilibrium with uniform stress and electric displacement. The tractions and charges on the lower crack surface are the negative of the tractions applied on the upper surface and thus

$$\begin{Bmatrix} T_1(x_1) \\ T_2(x_1) \\ T_3(x_1) \\ q(x_1) \end{Bmatrix}^{-} = -\begin{Bmatrix} T_1(x_1) \\ T_2(x_1) \\ T_3(x_1) \\ q(x_1) \end{Bmatrix}^{+} \tag{36}$$

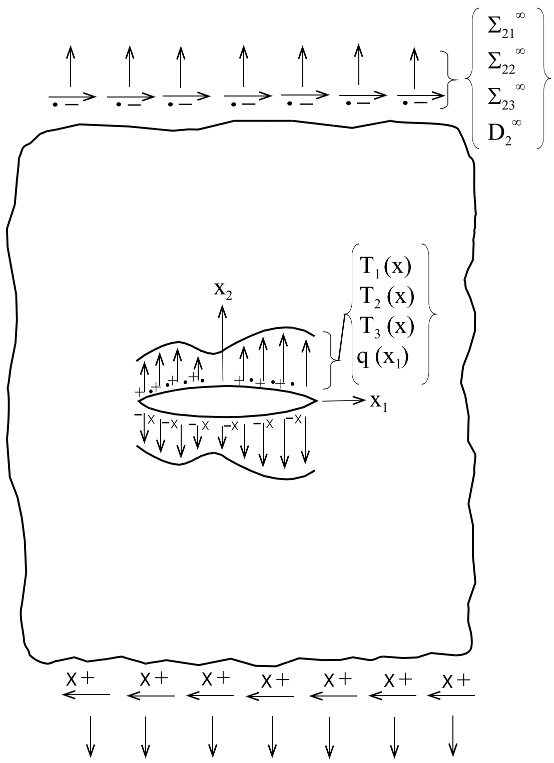

Fig. 5. A Griffith crack of length l with uniform stress and electric displacement at infinity plus tractions $T_i(x_1)$ and charges $q(x_1)$ applied to the crack surfaces.

where T_i is the traction applied to the crack surface, q is the charge per unit area attached to the crack surface and the superscript positive and negative signs denote the upper and lower crack surfaces, respectively.

In the absence of the crack, the stress and electric displacement everywhere have the values

$$\begin{Bmatrix} \Sigma_{21} \\ \Sigma_{22} \\ \Sigma_{23} \\ D_2 \end{Bmatrix} = \begin{Bmatrix} \Sigma_{21}^{\infty} \\ \Sigma_{22}^{\infty} \\ \Sigma_{23}^{\infty} \\ D_2^{\infty} \end{Bmatrix} \tag{37}$$

As a consequence, the problem shown in Fig. 5 can be replaced by the solution given by Eq. (37) plus the solution to a problem with zero loads and charges at infinity and the tractions and charges

$$\begin{Bmatrix} T_1(x_1) \\ T_2(x_1) \\ T_3(x_1) \\ q(x_1) \end{Bmatrix}^{+} + \begin{Bmatrix} \Sigma_{21}^{\infty} \\ \Sigma_{22}^{\infty} \\ \Sigma_{23}^{\infty} \\ -D_2^{\infty} \end{Bmatrix} \tag{38}$$

applied to the upper crack surface with the negative of these applied to the lower surface. It follows from Eqs. (8) and (31) that the intensity factors for the problem depicted in Fig. 5 are given by

$$\begin{Bmatrix} K_{\mathrm{II}} \\ K_{\mathrm{I}} \\ K_{\mathrm{III}} \\ K_{\mathrm{D}} \end{Bmatrix} = \frac{1}{\sqrt{\pi l/2}} \int_{-l/2}^{l/2} \sqrt{\frac{l/2 + x_1}{l/2 - x_1}} \left(\begin{Bmatrix} T_1(x_1) \\ T_2(x_1) \\ T_3(x_1) \\ -q(x_1) \end{Bmatrix}^{+} + \begin{Bmatrix} \Sigma_{21}^{\infty} \\ \Sigma_{22}^{\infty} \\ \Sigma_{23}^{\infty} \\ D_2^{\infty} \end{Bmatrix} \right) \mathrm{d}x_1 \tag{39}$$

where the equivalence between $T_i\mathrm{d}x_1$ and a line load and between $q\mathrm{d}x_1$ and a line charge has been used and integration performed to collect all the contributions from the upper and lower crack surfaces. The contribution from the loads and charges at infinity integrates readily and we obtain

$$\begin{Bmatrix} K_{\mathrm{II}} \\ K_{\mathrm{I}} \\ K_{\mathrm{III}} \\ K_{\mathrm{D}} \end{Bmatrix} = \begin{Bmatrix} \Sigma_{21}^{\infty} \\ \Sigma_{22}^{\infty} \\ \Sigma_{23}^{\infty} \\ D_2^{\infty} \end{Bmatrix} \sqrt{\pi l/2} + \frac{1}{\sqrt{\pi l/2}} \int_{-l/2}^{l/2} \sqrt{\frac{l/2 + x_1}{l/2 - x_1}} \begin{Bmatrix} T_1(x_1) \\ T_2(x_1) \\ T_3(x_1) \\ -q(x_1) \end{Bmatrix}^{+} \mathrm{d}x_1 \tag{40}$$

For the second example, we will consider PZT-5H poled in the x_2-direction. The material constants for this case are given in Appendix A. The relevant eigenvalue problem (Suo et al., 1992; Park and Sun, 1995; Kuna and Ricoeur, 2002) for this case has been solved and, as noted above, the eigenvalues p_i and the associated matrices $[H]$, $[A]$ and $[N]$ given also in Appendix A. These results can be combined with the general case Eq. (25) to explore the effect of a line load and a line charge placed at arbitrary locations relative to the crack tip. However, it is more instructive to investigate the near-tip behavior and thus use Eq. (33), which is valid for any crack in any geometry. The results for a line load of magnitude 1 N/m acting in the x_2-direction and a line of charges of magnitude 1 C/m both at an angle θ relative to the crack tip in the polar coordinate system of Fig. 1 have been computed numerically from Eq. (33) subject to the values given in Appendix A and the matrix in Eq. (34). The results for the line load are plotted in Fig. 6 and those for the line of charges in Fig. 7. Note that in contrast to the behavior when the tractions and charges are placed on the crack surface, the results in Fig. 6 show that a line force near the tip acting in the x_2-direction but not placed on the crack surface will produce non-zero intensity factor for all modes except III. Similarly, the results in Fig. 7 show that a line of charges placed near the crack tip but not on the crack surface will produce non-zero intensity factors for the stress Modes I and II as well as an electric displacement intensity factor.

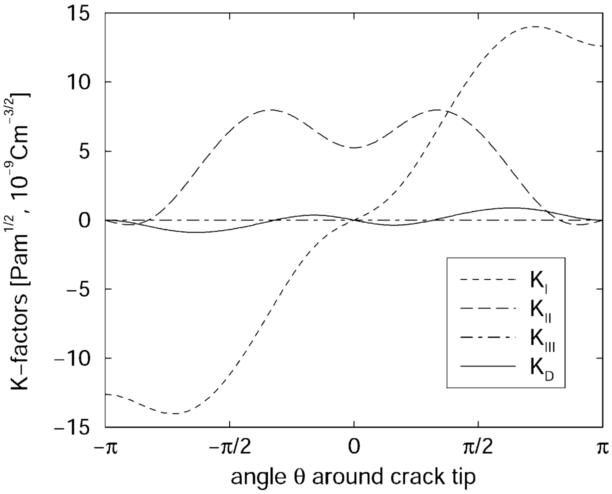

Fig. 6. Intensity factors for the crack tip in PZT-5H due to a near-tip line load P_2 equal to 1 N/m at an angle θ to the crack tip and at distance $r = 1$ mm from the crack tip. In this example, the crack is impermeable.

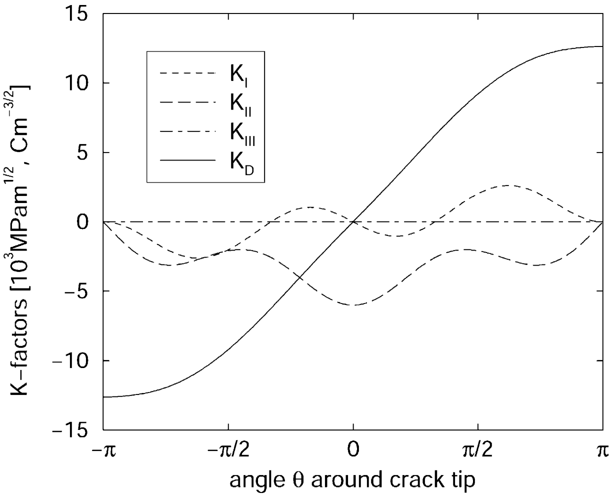

Fig. 7. Intensity factors for the crack tip in PZT-5H due to a near-tip line charge Q equal to 1 C/m at an angle θ to the crack tip and at distance $r = 1$ mm from the crack tip. In this example, the crack is impermeable.

5. The permeable crack

So far, the results we have obtained have all been focused on the impermeable crack for which the surface conditions are given by Eq. (4). As we have made clear, we do not accept this condition as physically realistic, but rather we have been using it as a convenience for the purposes of constructing our results. To deal with the permeable crack, we first observe that a generalization of the problem of a crack in an infinite body can be stated so that the interior of the crack sustains stresses and electric displacements given by

$$\{\Sigma^*\} = \begin{Bmatrix} \Sigma^*_{21}(x_1) \\ \Sigma^*_{22}(x_1) \\ \Sigma^*_{23}(x_1) \\ D^*_2(x_1) \end{Bmatrix} \tag{41}$$

where the superscript asterisk denotes the values within the crack. The stresses in the crack could be sustained by material inserted into it; e.g. a compliant rubber may be present in the crack or there may be bridging fibers or grains (Evans and McMeeking, 1986). We consider the case where the material transmitting the stress is non-conducting and therefore is a dielectric. Thus, the inserted material or the bridging fibers or grains are capable of sustaining an electric displacement. However, even when no solid material or bridging links are present within the crack, the interior is still capable of sustaining an electric displacement or equivalently an electric field. A case in point is an atmospheric gas or a non-conducting fluid, both of which will at least be weakly polarizable. In addition, the case of a vacuum within a crack pulled open by electromechanical or mechanical loads fits into our general picture. Although not polarizable, the vacuum within the space in the crack sustains an effective field $\kappa_0 E_2$, where κ_0 is the permittivity of free space. This field is the equivalent of an electric displacement and its continuity between the crack interior and the adjacent material will require in general that the electric field inside the crack is non-zero.

When these situations generating stress or electric displacement prevail within the crack in conjunction with no tractions or charges attached to the crack surfaces, continuity requires that the stress and electric displacement in the material immediately adjacent to the crack surfaces are given by Eq. (41). However, this condition of stress and electric displacement in the material adjacent to the crack surfaces can be produced simultaneously with zero stress and electric displacement within the crack by applying tractions and electric charge densities on the top surface of the crack given by

$$\{T^*\} = \begin{Bmatrix} -\Sigma^*_{21}(x_1) \\ -\Sigma^*_{22}(x_1) \\ -\Sigma^*_{23}(x_1) \\ D^*_2(x_1) \end{Bmatrix} \tag{42}$$

while the negative of these are applied on the bottom crack surface. Therefore, the intensity factors for a permeable crack (that may also transmit mechanical loads) can be computed from the weight function for an impermeable crack by using the expression in Eq. (42) as the tractions and charge densities in Eq. (40) being applied to the top surface of the crack. Thus the intensity factors for a permeable crack (and one that may also transmit bridging tractions) are given by

$$\begin{Bmatrix} K_{\mathrm{II}} \\ K_{\mathrm{I}} \\ K_{\mathrm{III}} \\ K_{\mathrm{D}} \end{Bmatrix} = \begin{Bmatrix} \Sigma^\infty_{21} \\ \Sigma^\infty_{22} \\ \Sigma^\infty_{23} \\ D^\infty_2 \end{Bmatrix} \sqrt{\pi l/2} - \frac{1}{\sqrt{\pi l/2}} \int_{-l/2}^{l/2} \sqrt{\frac{l/2 + x_1}{l/2 - x_1}} \begin{Bmatrix} \Sigma^*_{21}(x_1) \\ \Sigma^*_{22}(x_1) \\ \Sigma^*_{23}(x_1) \\ D^*_2(x_1) \end{Bmatrix} \mathrm{d}x_1 \tag{43}$$

This result is equivalent to those commonly used in the analysis of bridged cracks (Evans and McMeeking, 1986), but now the effect of electric fields has been included.

The difficulty remains that the electric displacement (and the bridging tractions) within the crack must somehow be computed. In general, this will require the solution of a boundary value problem that includes the imposition of the appropriate boundary conditions on the surfaces of the crack (Hao and Shen, 1994; McMeeking, 1999; Kemmer, 2000; Haug and McMeeking, 2000; McMeeking, 2001). Obtaining such a solution is not always a trivial step and when there is some complex electrical interaction across the crack (such as through contacting asperities), the analysis may be difficult and require numerical analysis. However, there are two simple cases that we can address. One is where the crack in a frictionless material is subject to sufficient compression so that its bottom and top surfaces are everywhere in intimate contact with each other. In that situation, the crack surface boundary conditions in terms of stress are that Σ_{21} and Σ_{23} are zero and Σ_{22} and D_2 are continuous across the crack and uniform along its length. This last assertion will be confirmed below. In addition, the displacement in the x_2-direction and the potential must be continuous across the crack. Since the stress and electric displacement inside the crack are all uniform, the displacement and potential differences across the crack are given by

$$\begin{Bmatrix} \Delta u_1(x_i) \\ \Delta u_2(x_i) \\ \Delta u_3(x_i) \\ \Delta\phi(x_i) \end{Bmatrix} = 4\sqrt{\frac{l^2}{4} - x_1^2}[H]\begin{Bmatrix} \Sigma_{21}^\infty - \Sigma_{21}^* \\ \Sigma_{22}^\infty - \Sigma_{22}^* \\ \Sigma_{23}^\infty - \Sigma_{23}^* \\ D_2^\infty - D_2^* \end{Bmatrix} \tag{44}$$

Given that Σ_{21}^* and Σ_{23}^* are zero, the requirement that Δu_2 and $\Delta\phi$ across the crack are zero provides

$$\begin{Bmatrix} \Sigma_{22}^* \\ D_2^* \end{Bmatrix} = \frac{1}{H_{22}H_{44} - H_{24}^2}\begin{bmatrix} H_{44} & -H_{24} \\ -H_{24} & H_{22} \end{bmatrix}\begin{bmatrix} H_{21} & H_{22} & H_{23} & H_{24} \\ H_{41} & H_{42} & H_{43} & H_{44} \end{bmatrix}\begin{Bmatrix} \Sigma_{21}^\infty \\ \Sigma_{22}^\infty \\ \Sigma_{23}^\infty \\ D_2^\infty \end{Bmatrix} \tag{45}$$

which confirms that the normal stress on the crack and the electric displacement in the crack are uniform. As a result of the above development, the intensity factors from Eq. (43) become

$$\begin{Bmatrix} K_{\mathrm{II}} \\ K_{\mathrm{I}} \\ K_{\mathrm{III}} \\ K_{\mathrm{D}} \end{Bmatrix} = \frac{1}{H_{22}H_{44} - H_{24}^2}\begin{bmatrix} H_{22}H_{44} - H_{24}^2 & 0 \\ H_{24}H_{41} - H_{21}H_{44} & H_{24}H_{43} - H_{23}H_{44} \\ 0 & H_{22}H_{44} - H_{24}^2 \\ H_{24}H_{21} - H_{22}H_{41} & H_{24}H_{23} - H_{22}H_{43} \end{bmatrix}\begin{Bmatrix} \Sigma_{21}^\infty \\ \Sigma_{23}^\infty \end{Bmatrix}\sqrt{\pi l/2} \tag{46}$$

where it can be seen that the applied shear stresses control the intensity factors. The Modes I and D intensity factors are non-zero only so that the displacement u_2 and the potential ϕ are continuous across that crack. Inspection of $[H]$ for PZT-5H poled in the x_2-direction as given in Appendix A indicates that both K_{I} and K_{D} are zero in that case.

The other simple case is when there is no mechanical connection across the crack and therefore all components of stress inside the flaw are zero. This implies that the loading in the problem is such that the crack surfaces are separated. In this case, it can be shown that the shape of the open crack is elliptical and the electric displacement inside the crack is uniform (Hao and Shen, 1994; Kemmer, 2000). This field uniformity can be understood with reference to the depolarization fields found within elliptical cavities in classical electrostatics (Jackson, 1962), extended to elasticity problems for elliptical cavities and inclusions by Eshelby (1957) and therefore valid for piezoelectric materials. Consequently, the intensity factors from Eq. (43) become

$$\begin{Bmatrix} K_{\mathrm{II}} \\ K_{\mathrm{I}} \\ K_{\mathrm{III}} \\ K_{\mathrm{D}} \end{Bmatrix} = \begin{Bmatrix} \Sigma_{21}^\infty \\ \Sigma_{22}^\infty \\ \Sigma_{23}^\infty \\ D_2^\infty - D_2^* \end{Bmatrix}\sqrt{\pi l/2} \tag{47}$$

where D_2^* is the uniform electric displacement within the crack. This latter term may be calculated from the observation that the boundary value problem is solved by Eq. (21) with D_2^∞ in that expression replaced by $D_2^\infty - D_2^*$. Of course, the result in Eq. (47) solves the problem of a crack in which the conditions adjacent to the crack surfaces are given by

$$\begin{Bmatrix} \Sigma_{21} \\ \Sigma_{22} \\ \Sigma_{23} \\ D_2 \end{Bmatrix} = -\begin{Bmatrix} \Sigma_{21}^{\infty} \\ \Sigma_{22}^{\infty} \\ \Sigma_{23}^{\infty} \\ D_2^{\infty} - D_2^{*} \end{Bmatrix} \tag{48}$$

and zero loads and electrical fields at infinity. To this must be added the solution with uniform stress and electric displacement for the infinite body without a crack. In this case, the difference across the crack surface in the resulting solution is given by Eq. (44) to be

$$\begin{Bmatrix} \Delta u_1(x_i) \\ \Delta u_2(x_i) \\ \Delta u_3(x_i) \\ \Delta \phi(x_i) \end{Bmatrix} = 4\sqrt{\frac{l^2}{4} - x_1^2}[H]\begin{Bmatrix} \Sigma_{21}^{\infty} \\ \Sigma_{22}^{\infty} \\ \Sigma_{23}^{\infty} \\ D_2^{\infty} - D_2^{*} \end{Bmatrix} \tag{49}$$

and therefore, the field in the x_2-direction everywhere in the crack interior is (Kemmer, 2000).

$$E_2^{*} = -\frac{H_{4i}\Sigma_{2i}^{\infty} + H_{44}(D_2^{\infty} - D_2^{*})}{H_{2i}\Sigma_{2i}^{\infty} + H_{24}(D_2^{\infty} - D_2^{*})} \tag{50}$$

where Einstein repeated index summation convention is used in the range 1–3. Hao and Shen (1994) use essentially the same formulation as is stated in Eq. (50), but present it as a local relationship at x_1 for the capacitance of the space within the crack as a function of the crack opening. Kemmer (2000), however, recognizes that the field within the Griffith crack is uniform and thus is able to deduce Eq. (50).

Now let the interior of the crack have permittivity κ_0, which, as before, can be assumed to be the value for free space since most gases are not greatly polarizable. Thus the electric displacement in the crack is given by $\kappa_0 E_2^{*}$ and for anisotropic materials, the quadratic equation arising from Eq. (50) leads to the result

$$D_2^{*} = \frac{1}{2H_{24}}\left[H_{2i}\Sigma_{2i}^{\infty} + H_{24}D_2^{\infty} - \kappa_0 H_{44} - \sqrt{(\kappa_0 H_{44} - H_{2i}\Sigma_{2i}^{\infty} - H_{24}D_2^{\infty})^2 + 4\kappa_0 H_{24}(H_{4i}\Sigma_{2i}^{\infty} + H_{44}D_2^{\infty})}\right] \tag{51}$$

where the other solution has been dispensed with on the grounds given by Kemmer (2000) that it involves a negative crack opening displacement. Hao and Shen (1994) provide a numerical result equivalent to Eq. (51). The expression in Eq. (51) is invalid for isotropic materials where $[H]$ is diagonal. For the isotropic case, Eq. (51) is replaced by

$$D_2^{*} = \frac{D_2^{\infty}}{1 + \frac{2(1 - v^2)\kappa \Sigma_{22}^{\infty}}{\kappa_0 Y}} \tag{52}$$

where v is Poisson's ratio, κ is the dielectric permittivity of the material and Y is Young's modulus. Note that in Eq. (52), the isotropic results $H_{22} = (1 - v^2)/Y$ and $H_{44} = -1/2\kappa$ have been used.

The expression in Eq. (51) for anisotropic materials and that in Eq. (52) for isotropic materials can be inserted into Eq. (47) to give the intensity factors in terms of the mechanical and electrical loading at infinity. The result is a rather complex formula. A limiting case may be studied to yield some insight. When the applied mechanical and electrical loads are uniformly small, Eq. (51) linearizes to give

$$D_2^{*} = \frac{1}{H_{44}}[H_{4i}\Sigma_{2i}^{\infty} + H_{44}D_2^{\infty}] \tag{53}$$

which is valid also as a linearization of Eq. (52) for the isotropic case since H_{4i} are all zero in that case. The general linearized result for the electric displacement intensity factor from Eq. (47) is then

$$K_{\mathrm{D}} = -\frac{H_{4i}\Sigma_{2i}}{H_{44}}\sqrt{\pi l/2} \tag{54}$$

It should be noted that H_{44} is negative, so that for tensile stress, the result for K_{D} will be positive. Note that Eq. (54) is valid for the isotropic case but indicates that K_{D} is zero in this situation. (N.B. The latter result arises because the off-diagonal terms in the Irwin matrix are zero when the material is isotropic and the Einstein summation implied in Eq. (54) ranges over the subscripts from 1 to only 3.) The linearized result in Eq. (54) in general is in fact the solution for K_{D} when the crack opening is zero. It enforces the condition that there should be no potential difference across the crack in that situation since the crack surfaces are in contact with each other. This can be confirmed by comparing Eq. (53) with Eq. (49) with $\Delta\phi$ set to zero. Such a situation is appropriate to first order for a crack with a very small crack opening as arises in the linearized case with small applied mechanical and electrical loads. Thus, the linearized version of this example is a special case of the previous situation that was illustrated where the crack surfaces are closed due to compression and the normal stress across the crack is non-zero.

6. Closure

The weight function for a Griffith crack in a piezoelectric material has been derived. The weight function provides a means of calculating the intensity factors for the crack when arbitrary loads and electrical charges are imposed, given that the loads and charges have an equilibrium distribution. The method for deriving the weight function has been given for the Griffith crack for clarity. However, the procedure presented can be used for a crack of any shape in any body, finite or infinite. Therefore, in principle, we have derived the weight function for all piezoelectric specimens.

Note that strictly, we have derived the weight function for a crack that is impermeable to the electric field. However, judicious use of the weight function with charge distributions on the crack surface allows us to obtain the intensity factors for a body containing a permeable crack. In this way, we can overcome the limitation that would otherwise confine the weight function to applications involving the non-physical example of an impermeable crack.

Acknowledgements

The contribution of RM to this research was supported by the US National Science Foundation through the Grant CMS 9813022. The contribution of AR was supported by the Deutsche Forschungsgemeinschaft as part of a research program on Multifunctional Ceramics.

Appendix A

Here we give the material constants, the eigenvalues p_i, the Irwin matrix $[H]$ and the matrices $[A]$ and $[N]$ for PZT-5H with the positive x_2-axis as the poling direction.

The constitutive matrices can be written in Voigt form for the global coordinate system such that

$$\begin{Bmatrix} \Sigma_{11} \\ \Sigma_{22} \\ \Sigma_{33} \\ \Sigma_{23} \\ \Sigma_{13} \\ \Sigma_{12} \end{Bmatrix} = \begin{bmatrix} c_{11} & c_{13} & c_{12} & 0 & 0 & 0 \\ c_{13} & c_{33} & c_{13} & 0 & 0 & 0 \\ c_{12} & c_{13} & c_{11} & 0 & 0 & 0 \\ 0 & 0 & 0 & c_{44} & 0 & 0 \\ 0 & 0 & 0 & 0 & \frac{c_{11}-c_{12}}{2} & 0 \\ 0 & 0 & 0 & 0 & 0 & c_{44} \end{bmatrix} \begin{Bmatrix} \varepsilon_{11} \\ \varepsilon_{22} \\ \varepsilon_{33} \\ 2\varepsilon_{23} \\ 2\varepsilon_{13} \\ 2\varepsilon_{12} \end{Bmatrix} - \begin{bmatrix} 0 & e_{31} & 0 \\ 0 & e_{33} & 0 \\ 0 & e_{31} & 0 \\ 0 & 0 & e_{15} \\ 0 & 0 & 0 \\ e_{15} & 0 & 0 \end{bmatrix} \begin{Bmatrix} E_1 \\ E_2 \\ E_3 \end{Bmatrix} \tag{A.1}$$

$$\begin{Bmatrix} D_1 \\ D_2 \\ D_3 \end{Bmatrix} = \begin{bmatrix} 0 & 0 & 0 & 0 & 0 & e_{15} \\ e_{31} & e_{33} & e_{31} & 0 & 0 & 0 \\ 0 & 0 & 0 & e_{15} & 0 & 0 \end{bmatrix} \begin{Bmatrix} \varepsilon_{11} \\ \varepsilon_{22} \\ \varepsilon_{33} \\ 2\varepsilon_{23} \\ 2\varepsilon_{13} \\ 2\varepsilon_{12} \end{Bmatrix} + \begin{bmatrix} \kappa_{11} & 0 & 0 \\ 0 & \kappa_{33} & 0 \\ 0 & 0 & \kappa_{11} \end{bmatrix} \begin{Bmatrix} E_1 \\ E_2 \\ E_3 \end{Bmatrix} \tag{A.2}$$

where c_{ij} are elastic moduli, ε_{ij} are strain components, e_{ij} are piezoelectric coefficients, E_i are electric field components and κ_{ij} are dielectric permittivities. Specific values for PZT-5H are

$$\begin{aligned} &c_{11} = 12.6 \times 10^{10}\ \text{Pa}, \quad c_{12} = 5.5 \times 10^{10}\ \text{Pa}, \quad c_{13} = 5.3 \times 10^{10}\ \text{Pa}, \\ &c_{33} = 11.7 \times 10^{10}\ \text{Pa}, \quad c_{44} = 3.53 \times 10^{10}\ \text{Pa} \\ &e_{31} = -6.5 \times 10^{9}\ \text{N/(GV m)}, \quad e_{33} = 23.3 \times 10^{9}\ \text{N/(GV m)}, \quad e_{15} = 17.0 \times 10^{9}\ \text{N/(GV m)} \\ &\kappa_{11} = 15.1 \times 10^{9}\ \text{N/(GV)}^2, \quad \kappa_{33} = 13.0 \times 10^{9}\ \text{N/(GV)}^2 \end{aligned} \tag{A.3}$$

The eigenvalues obtained for solving the plane problem in x_1–x_2 space in PZT-5H with the poling direction being x_2 are

$$\begin{aligned} p_1 &= -0.193165 + 1.037274\text{i} \\ p_2 &= 0.193165 + 1.037274\text{i} \\ p_3 &= 1.071040\text{i} \\ p_4 &= 1.002829\text{i} \end{aligned} \tag{A.4}$$

It should be noted that the eigenvalues come in conjugate pairs. However, only the eigenvalues having positive imaginary part have been given above.

The columns of the matrix $[A]$ represent eigenvectors corresponding to the four eigenvalues given in Eq. (A.4). For the case studied, this matrix is

$$[A] = \begin{bmatrix} 0.259185 + 1.434640\text{i} & -0.259185 + 1.434640\text{i} & -0.395612\text{i} & 0 \\ -1.109441 + 0.703125\text{i} & -1.109441 - 0.703125\text{i} & 0.476599 & 0 \\ 0 & 0 & 0 & 1 \\ -1 & -1 & -1 & 0 \end{bmatrix} \tag{A.5}$$

where the units used to compute this matrix are: force N; length m; electrical potential GV. Thus, using these matrices, stress is computed in Pa, electric field in GV/m, electric displacement in nC/m^2, stress intensity factors in Pa$\sqrt{\text{m}}$, electric displacement factors in nC/m$^{3/2}$ and energy release rates in J/m^2.

It should be noted that the eigenvectors embedded as columns in the matrix $[A]$ satisfy the orthogonality conditions of Ting (1986) (i.e. his Eq. (3.10)). However, we have not taken the additional optional step of normalizing the eigenvectors according to Ting's (1986) Eq. (3.11). Therefore, our results do not satisfy the orthogonality conditions given as his Eq. (3.15) by Ting (1986) nor the closure relationships in Ting's (1986) Eq. (3.17). However, the failure to satisfy these conditions through our choice not to normalize the eigenvectors is not a deficiency of our results and any effect is compensated by the values presented for the matrix $[N]$ given below. This is obvious once it is noted that in all of our results Eqs. (21)–(27), the effect of $[A]$ and $[N]$ always appears in terms of their product.

Given the value for $[A]$ above, the matrix $[N]$ is then

$$[N] = \begin{bmatrix} -0.088609+0.223461\mathrm{i} & -0.251752-0.041766\mathrm{i} & 0 & 0.006037-0.025832\mathrm{i} \\ -0.088609-0.223461\mathrm{i} & 0.251752-0.041766\mathrm{i} & 0 & -0.006037-0.025832\mathrm{i} \\ 0.093798 & 0.211285\mathrm{i} & 0 & -0.406129\mathrm{i} \\ 0 & 0 & -0.282487\mathrm{i} & 0 \end{bmatrix} \times 10^{-10} \tag{A.6}$$

and the Irwin matrix is given uniquely by

$$[H] = \begin{bmatrix} 0.877585 & 0 & 0 & 0 \\ 0 & 0.803275 & 0 & 0.638765 \\ 0 & 0 & 1.412435 & 0 \\ 0 & 0.638765 & 0 & -2.288973 \end{bmatrix} \times 10^{-11} \tag{A.7}$$

References

Bueckner, H.F., 1970. A novel principle for the computation of stress intensity factors. Zeitschrift für Angewandte Mathematik und Mechanik 50, 529–546.

Bueckner, H.F., 1973. Field singularities and related integral representations. Mechanics of Fracture 1, 239–314.

Eshelby, J.D., 1957. The determination of the elastic field of an ellipsoidal inclusion and related problems. Proceedings of the Royal Society of London A241, 376–396.

Eshelby, J.D., Read, W.T., Shockley, W., 1953. Anisotropic elasticity with applications to dislocation theory. Acta Metallurgica 1, 251.

Evans, A.G., McMeeking, R.M., 1986. On the toughening of ceramics by strong reinforcements. Acta Metallurgica 34, 2435–2441.

Hao, T.H., Shen, Z.Y., 1994. A new electric boundary condition of electric fracture mechanics and its applications. Engineering Fracture Mechanics 47, 793–802.

Haug, A., McMeeking, R.M., 2000. Energy release rate for a crack with extrinsic surface charge in a piezoelectric compact tension specimen. In: Chuang, T.-J., Rudnicki, J.W. (Eds.), Multiscale Deformation and Fracture in Materials and Structures. Kluwer, Dordrecht, pp. 349–359.

Jackson, J.D., 1962. Classical Electrodynamics. Wiley, New York.

Kemmer, G., 2000. Berechnung von elektromechanischen Intensitatsparametern bei Rissen in Piezokeramiken. Ph.D. Dissertation. Technische Universität Dresden, Fortschrittberichte VDI Reihe 18 No. 261. VDI Verlag, Dusseldorf, Germany.

Kuna, M., Ricoeur, A., 2002. Theoretical investigation of the fracture behavior in ferroelectric ceramics. In: Bradt, R.C. et al. (Eds.), Fracture Mechanics of Ceramics, vol. 13. Kluwer, Dordrecht, pp. 63–82.

Labbens, R.C., Heliot, J., Pellisier-Tanon, A., 1976. Weight functions for three-dimensional crack problems. In: Cracks and Fracture. In: ASTM STP, 601. ASTM, Philadelphia, pp. 448–467.

Labbens, R.C., Pellisier-Tanon, A., Heliot, J., 1975. Practical method for calculation stress intensity factors through weight functions. In: Mechanics of Crack Growth. In: ASTM STP, 590. ASTM, Philadelphia, pp. 368–385.

Ma, L.-F., Chen, Y.-H., 2001. Weight functions for interface cracks in dissimilar anisotropic piezoelectric materials. International Journal of Fracture 110, 263–279.

Marshall, D.B., Cox, B.N., Evans, A.G., 1985. The mechanics of matrix cracking in brittle-matrix fiber composites. Acta Metallurgica 33, 2013–2021.

McMeeking, R.M., 1999. Crack tip energy release rate for a piezoelectric compact tension specimen. Engineering Fracture Mechanics 64, 217–244.

McMeeking, R.M., 2001. Towards a fracture mechanics for brittle piezoelectric and dielectric materials. International Journal of Fracture 108, 25–41.

Paris, P.C., McMeeking, R.M., 1975. Efficient finite element methods for stress intensity factors using weight function. International Journal of Fracture 11, R354–356.

Paris, P.C., McMeeking, R.M., Tada, H., 1976. The weight function method for determining stress intensity factors. In: Cracks and Fracture. In: ASTM STP, 601. ASTM, Philadelphia, pp. 471–489.

Park, S.B., Sun, C.T., 1995. Effect of electric field on fracture of piezoelectric ceramics. International Journal of Fracture 70, 203–216.
Parks, D.M., Kamenetzky, E.M., 1979. Weight functions from virtual crack extension. International Journal for Numerical Methods in Engineering 14, 1693–1706.
Rice, J.R., 1972. Some remarks on elastic crack-tip stress fields. International Journal for Solids and Structures 8, 751–758.
Suo, Z., Kuo, C.M., Barnett, D.M., Willis, J.R., 1992. Fracture mechanics for piezoelectric ceramics. Journal of the Mechanics and Physics of Solids 40, 739–765.
Vanderglas, M.L., 1978. A stiffness derivative finite element technique for determination of influence functions. International Journal of Fracture 14, R291–294.